Corrections for Pumped SBE 41CP CTDs Determined from Stratified Tank Experiments

KIM I. MARTINI AND DAVID J. MURPHY

Sea-Bird Scientific, Bellevue, Washington

RAYMOND W. SCHMITT

Woods Hole Oceanographic Institution, Woods Hole, Massachusetts

NORDEEN G. LARSON

Sea-Bird Scientific, Bellevue, Washington

(Manuscript received 26 March 2018, in final form 6 December 2018)

ABSTRACT

Sea-Bird Scientific SBE 41CP CTDs are used on autonomous floats in the global Argo ocean observing program to measure the temperature and salinity of the upper ocean. While profiling, the sensors are subject to dynamic errors as they profile through vertical gradients. Applying dynamic corrections to the temperature and conductivity data reduces these errors and improves sensor accuracy. A series of laboratory experiments conducted in a stratified tank are used to characterize dynamic errors and determine corrections. The corrections are adapted for Argo floats, and recommendations for future implementation are presented.

1. Introduction

The Argo array is a global ocean observation program made up of >3800 autonomous, freely drifting profiling floats. The goal of this program is monitor and detect changes to the physical properties of the upper ocean with unprecedented spatial coverage. This requires sensors that can accurately and reliably measure the temperature, salinity, and pressure of seawater over multiyear deployments. More than 95% of Argo floats are deployed with Sea-Bird Scientific (i.e., Sea-Bird Electronics, Inc.) SBE 41CP CTDs sampling at 1 Hz that adhere to static accuracy specifications of ±0.002°C, ±0.002 Practical Salinity Scale of 1978 (PSS-78), and ±2 dbar to accomplish this. As with all sensors, accuracy is affected by dynamic changes in the marine environment. By characterizing dynamic errors and determining corrections, the overall accuracy of returned data is improved, benefiting the Argo observational program.

The SBE 41CP CTD consists of a thermistor to measure temperature, a Druck (GE Baker Hughes) or Kistler Instrument Corp. strain gauge to measure pressure, and a borosilicate glass cell to measure conductivity. A duct connects the temperature and conductivity sensors, and seawater is pumped through the plumbing at a constant rate. By controlling the flow rate, the same parcel of water can be measured by plumbed sensors, reducing salinity spiking and improving accuracy. Practical salinity is then directly calculated on board the float from measured temperature and salinity. Temperature, pressure, and practical salinity are averaged over 1–2-m bins to reduce data transmission volume before being telemetered back to shore.

There are two primary types of errors that affect data accuracy in CTDs: static and dynamic errors. Static errors are observed in equilibrated conditions. In Sea-Bird CTDs, static errors are caused by sensor and electronic drift. Corrections to static errors are determined in the

Denotes content that is immediately available upon publication as open access.

Supplemental information related to this paper is available at the Journals Online website: https://doi.org/10.1175/JTECH-D-18-0050.s1.

Corresponding author: Kim I. Martini, kmartini@seabird.com

DOI: 10.1175/JTECH-D-18-0050.1

laboratory during predeployment calibrations against known standards. Dynamic errors are observed in changing conditions. Dynamic errors are caused by sensor response times, sensitivity to changes in the marine environment, and the rate limits of electronics. Corrections to dynamic errors are determined from in situ data or controlled laboratory experiments and applied to the data in postprocessing. Dynamic errors are reduced in the Sea-Bird CTDs by employing a pump, which controls flow rates and reduces environmental change near the sensor.

Dynamic corrections to CTD data have been determined for SBE 3 temperature and SBE 4 conductivity sensors used on Sea-Bird 911plus profiling systems (Lueck 1990; Morison et al. 1994) and for the SBE 41CP deployed on ice tethered profilers (ITPs) in the Arctic (Johnson et al. 2007). These corrections are sensitive to differences in plumbing, pump speed, cell geometry, and profiling speed. Average profiling speeds in Argo floats are slower in than in ITPs, 0.1 and 0.3 $\mathrm{m\,s^{-1}}$, respectively. Therefore, corrections for Argo floats must be adjusted accordingly. Salinity returned from the floats is bin averaged, and cannot be used to determine the corrections. Therefore, additional in situ or laboratory profiling experiments returning unbinned 1-Hz data must be conducted to determine the appropriate corrections.

In this paper, dynamic errors and their corrections for SBE 41CP CTDs are determined in a series of laboratory experiments. By profiling CTD sensors through a known vertical temperature and salinity gradient, their response can be characterized and the appropriate correction determined. The types of errors that can affect CTD data are described and techniques used to determine their corrections are discussed. The corrections are then adjusted to reflect in situ sampling.

As of the writing of this paper, dynamic corrections are not applied to SBE 41P CTDs deployed on Argo profiling floats. The laboratory experiments presented here are used to understand SBE 41CP CTD sensor response and determine which corrections will lead to the largest improvements for Argo data. Although correction coefficients are presented, they may not be directly applicable in situ. The analysis is intended to serve as a guideline for determining in situ corrections to SBE 41CP CTD data and implementing them on board Argo floats in the future.

2. Dynamic errors in pumped CTD systems

There are three types of dynamic errors that can be corrected before derived oceanographic variables such as salinity and density are calculated:

1) thermistor thermal mass τ_T,
2) time lag between temperature and conductivity due to the physical separation of the sensors t_p, and
3) conductivity cell thermal mass α and τ_{CTM}.

The corrections must be made in the order listed above, because the efficacy of each depends on the accuracy of the former. These errors and their corrections are discussed in the following sections.

a. Thermistor thermal mass

Thermistors are well suited for measuring temperature in the ocean due to their small size and fast response times. Although thermistors have a fast response, they are still subject to dynamic errors caused by the time it takes for heat to be transferred from seawater to the thermistor, manifesting as a lag. Heat transfer between seawater and the thermistor is affected by the fluid boundary layer around the tip of the probe and the conduction of heat through the metal housing that surrounds the thermistor bead, that is, the thermistor thermal mass.

Following Fofonoff et al. (1974), the thermal mass lag response can be modeled as

$$T = T_m + \tau_T(dT_m/dt), \tag{1}$$

where T is the true seawater temperature, T_m is the temperature recorded by the thermistor, and τ_T is the response time of the thermistor. The response time τ_T is dependent on the speed of the fluid past the probe. For a pumped system with constant fluid velocity τ_T is constant, but it changes with profiling speed in unpumped systems.

b. Temperature and conductivity time lag

Derived seawater properties such as salinity and density must be calculated from the same parcel of water. If not, spiking can occur. Spiking, spuriously large values of salinity, is caused by the temporal mismatch of the temperature and conductivity data.

By employing a pump on the SBE 41CP to draw seawater through the temperature–conductivity (TC) duct, the rate at which water travels past the sensors is constant. The time it takes for a parcel of water to travel from the thermistor to the conductivity cell is therefore also constant. By calculating the travel time, temperature and conductivity data can be temporally aligned, eliminating most salinity spiking. In practice, alignment can be achieved by lagging the conductivity relative to temperature when sampled simultaneously.

c. Conductivity cell thermal mass

In CTDs with a glass conductivity cell, measured conductivity is a function of the salinity of seawater within the cell and the temperature of the cell itself. Due to the

cell's thermal mass, the temperature of the glass differs from the temperature of the seawater within the cell. If not accounted for, the temperature difference between seawater and glass leads to dynamic errors that degrade salinity accuracy. The cell thermal mass error appears similar to an increase in the conductivity response time. For example, if the float is profiling through a step increase (decrease) in temperature, it will take a finite time for the measured conductivity to approach the true conductivity as the cell temperature warms (cools).

Cell thermal mass can be corrected by adjusting the conductivity so there is no thermal lag (Lueck 1990) or adjusting the seawater temperature to represent the temperature of the glass cell (Morison et al. 1994). The method proposed by Lueck (1990) is used in the Sea-Bird data processing software. Here we use the method proposed by Morison et al. (1994). Coefficients determined using either method are identical, but the Morison et al. (1994) method is computationally more efficient and easier to apply on board profiling floats.

The thermal response of the conductivity cell is dependent on heat transfer between seawater and glass at the interior of the cell wall, heat conduction through the glass cell and urethane coating, and heat transfer at the outer wall of the cell. A step change in temperature from 0° to 1°C passing through the cell at time t can be described by the Heaviside step function $H(t)$. Following Lueck (1990) and Johnson et al. (2007), the difference in the temperature between the inner surface of the cell T_c and the fluid within the cell T_w as the step passes through the cell can be approximated by

$$T_w - T_c = \alpha H(t) e^{-t/\tau_{\mathrm{CTM}}}, \tag{2}$$

where $T_w = 1$. The equation represents a step change in temperature as an initial response, which relaxes as an exponential decay to the final temperature as heat conducts through the cell wall. The coefficient α is the magnitude of the error. The coefficient τ_{CTM} is the thermal mass time scale: the relaxation time for the exponential decay. Both α and τ_{CTM} are dependent on the flow speed within the cell, which changes with the flushing time of the cell, the size of the thermal boundary layer on the wall of the cell, and heat conduction and convection at the cell wall boundaries.

3. Experiment description

a. Stratified tank setup

Dynamic corrections to the SBE 41CP CTD are determined from a series of profiling experiments conducted in the stratified tank at the Woods Hole Oceanographic Institution (WHOI). The WHOI stratified tank contains a stable two-layer fluid (Schmitt et al. 2005), with a cold and fresh layer at the surface (~20°C; ~1 PSU) and a warm and salty layer at the bottom (~26°C; ~16 PSU) (Fig. 1). At the diffusive interface between the two layers is a sharp, ~10-cm-thick temperature and salinity gradient. The temperature interface is 15% thicker than the salinity interface due to the larger molecular diffusivity of heat ($D_T \approx 10^{-7}\,\mathrm{m^2\,s^{-1}}$) than salt ($D_T \approx 10^{-9}\,\mathrm{m^2\,s^{-1}}$).

For the experiment, the SBE 41CP was dropped vertically through the tank to simulate an Argo float profile. The CTD was modified to fit in a compact housing connected to a hanging cable and lowered downward into the tank. In the downward orientation, the opening of the TC duct is in the direction of flow and the encountered fluid is undisturbed by the passage of the instrument. For comparison, the SBE 41CP is pointed upward on the top of Argo floats and samples while ascending. Between each profile, the interface was checked for waves and disturbances caused by the passage of the instrument package. Only when the interface had settled completely was the next profile made. The cable was paid out by the tank winch at 0.05, 0.10, and 0.15 $\mathrm{m\,s^{-1}}$. A modified circuit board was used to increase the sampling rate from 1 to 16 Hz to fully resolve gradients in the interface. The three ASCII data files used in this analysis are included as online supplemental material and can be read with any text editor.

b. Thermistor interference

The temperature data were contaminated by periodic noise that may have been caused by electromagnetic interference from inside the tank (Fig. 2). A first-order 3–4-Hz Butterworth stop filter was applied to the data to remove the oscillation and retain higher-frequency variability. A single-pole, low-pass filter with a cutoff of 4 Hz identical to that used by the Sea-Bird data processing software was also tested. This filter was not used because it changed the shape of the profile significantly, mimicking a change in sensor response time that affected the determination of the correction coefficients.

c. Sampling mode

When profiling, the SBE 41CP can be operated in spot-sample mode to conserve battery power or continuous-sampling mode for finer vertical resolution. During a spot sample, the pump is turned on for 2.5 s to flush the sensors with fresh seawater at a flow rate of 40 $\mathrm{ml\,s^{-1}}$ after which a single temperature, pressure, and conductivity sample is taken. Because of the short duration of flow through the cell, dynamic corrections are not applied to the spot-sampled data. During the continuous-sampling mode, the pump stays on and seawater is continuously pumped through the system at a rate of 10 $\mathrm{ml\,s^{-1}}$.

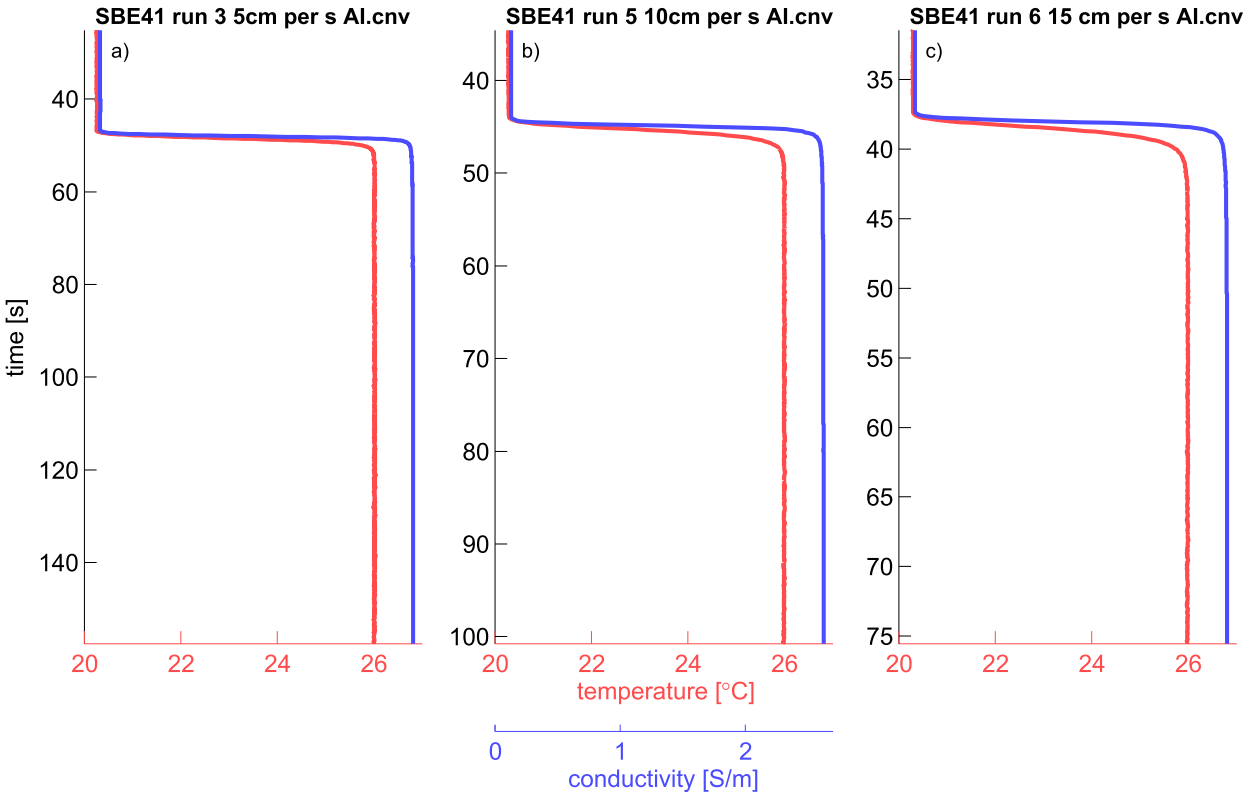

FIG. 1. Raw temperature (red curves) and conductivity (blue curves) data from the pumped SBE 41CP profiling downward at (a) 0.05, (b) 0.10, and (c) 0.15 m s^{-1}. The data have been cropped to exclude data taken at the top before profiling and after the unit reached the bottom of the tank.

This corresponds to a fluid velocity of 2 m s^{-1} through the 4-mm-diameter conductivity cell, completely flushing the 14-cm-long cell in 2 ms. The SBE 41CP was operated in continuous mode in the stratified tank, and therefore dynamic corrections presented here are only applicable when the CTD is operating in continuous mode.

4. Determining the correction coefficients

The correction coefficients are determined here for the Sea-Bird SBE 41CP CTD sampling at 16 Hz. Coefficients for in situ CTDs deployed on floats sampling at 1 Hz are different than when sampling at 16 Hz and are determined in section 5.

a. Thermistor thermal mass correction

To determine the thermal mass correction for the thermistor, the known shape of an interface that is dominated by diffusion is exploited (Fig. 3a). In a purely diffusive system, the temperature gradient between two regions of constant temperature can be described by the error function, whose vertical derivative is a Gaussian function that is symmetric about the center of the interface. Therefore, if the appropriate thermal mass correction is applied, the first difference of the temperature profile should also be a Gaussian function that is symmetric about the center of the interface. By testing the symmetry of the temperature vertical derivative while iterating through a range of lag times, we can find the optimal thermal mass coefficient τ_T.

Interface symmetry was estimated by taking the first difference of the temperature profile, folding it along the interface center, and minimizing the difference between the upper and lower parts of the thermal gradient in the interface (Fig. 3). Before folding, the temperature first difference was smoothed with a 7-point boxcar filter to reduce noise.

For a perfectly diffusive interface, the difference between the upper and lower portions is zero when the correct time constant is applied. In the stratified tank, the interface is modified by convective instabilities, as well as fluid entrainment caused by the passage of the CTD and instrument noise. Although these contributions are small, the interface will never be perfectly symmetric. Therefore, the optimal time constant is determined by minimizing the difference between the upper and lower thermal gradient. The center of the interface is defined as the maximum temperature gradient and recalculated for

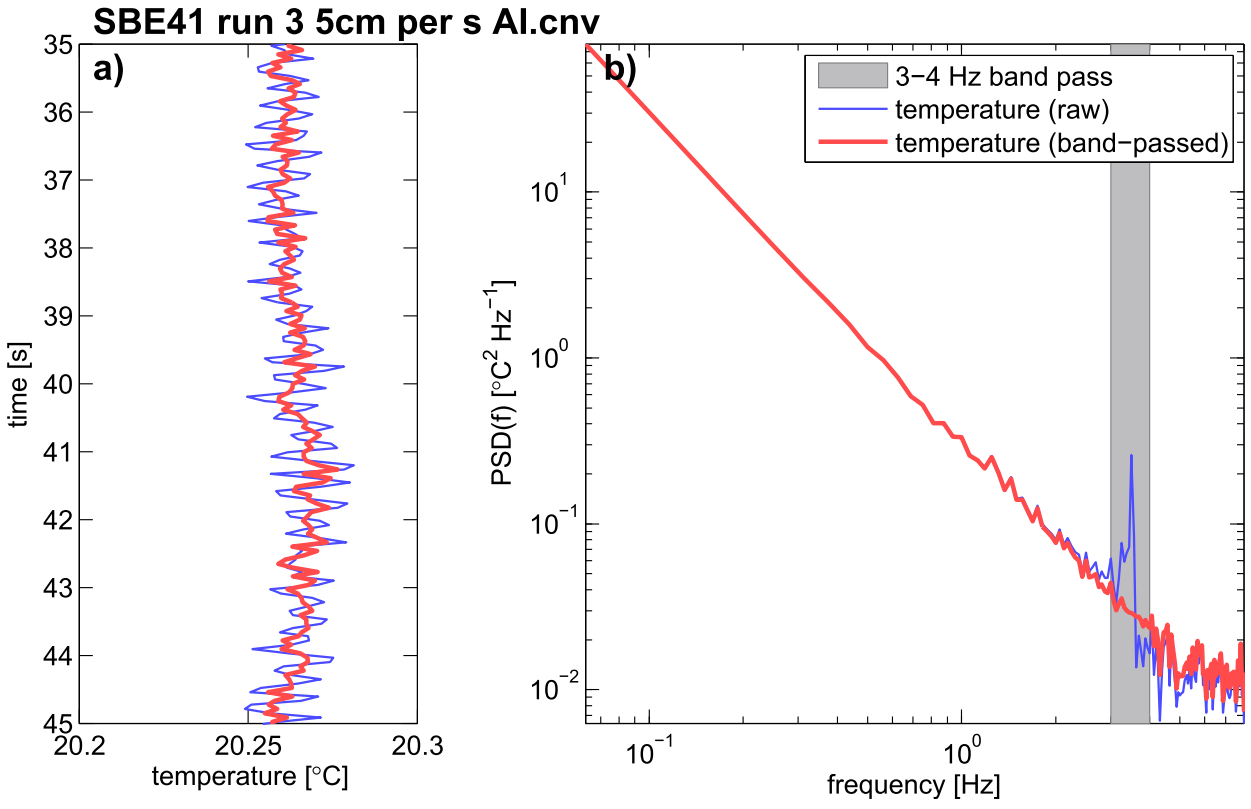

FIG. 2. (a) Interference in the tank causes temperature to oscillate at a frequency between 3 and 4 Hz (blue curve) that can be removed by applying a Butterworth bandpass filter (red curve). (b) Spectral analysis reveals the peak in the unfiltered data, with the peak (blue curve), the 3–4-Hz bandpass filter (gray shading), and the filtered data (red curve). Filtering removes the peak but keeps higher-frequency variability.

each iteration. Time constants tested range from 0 to 1 s. If the time constant was set too high, temperature in the interface can exceed temperatures in the lower layer which is physically unrealistic. Therefore, a second constraint was also applied: the temperature in the interface could not exceed the temperature in the lower layer.

Optimized time constants sharpen the interface, increase the maximum temperature gradient, and reduce the interface thickness (Fig. 3). Thermistor time constants are within ±0.03 s, smaller than the 0.0625-s sampling interval, and indicate the thermistor thermal mass time correction is relatively insensitive to changes in profiling speed observed on Argo floats (Table 1).

b. *Temperature and conductivity alignment*

Temperature and conductivity are typically aligned by adjusting the time lag to minimize salinity spiking or aligning their gradients in spectral space (Horne and Toole 1980). Although these techniques have been effectively used in oceanic data, they cannot be used in the stratified tank as instrument noise is larger than the vertical gradients found in the well-mixed upper and lower layers. Instead, vertical gradients at the interface are utilized to align the temperature and conductivity profiles. When the profiles are aligned, so are the interface centers (and depth). The interface center is defined to be the maximum vertical gradient and the lag is the difference in scans between the maxima. Conductivity lags temperature by 0, 1, and 1 scans for the 0.05, 0.10, and 0.15 m s^{-1} profiles, respectively (Table 1).

c. *Conductivity cell thermal mass correction*

Dynamic errors caused by cell thermal mass are corrected following the method proposed by Morison et al. (1994). In Morison et al. (1994), the temperature is corrected to represent the true temperature of seawater within the glass conductivity cell. The results of the correction are identical to Lueck (1990), where the conductivity rather than the temperature is adjusted. The correction is applied to the temperature profile using the recursive formula

$$T_T(n) = -bT_T(n-1) + a[T(n) - T(n-1)], \quad (3)$$

where $T_T(n)$ is the corrected temperature of seawater within the conductivity cell and $T(n)$ is the uncorrected

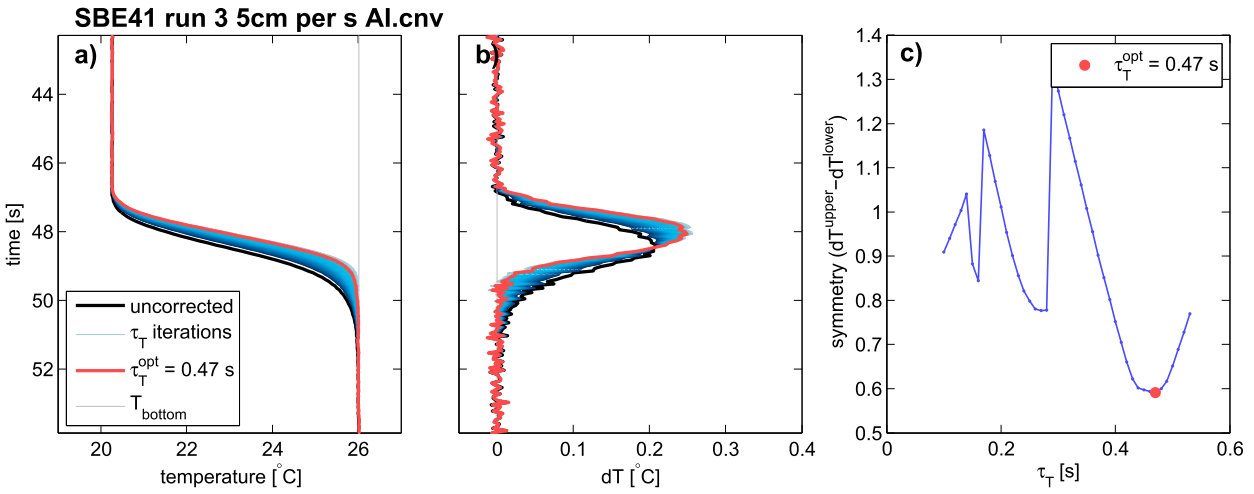

FIG. 3. (a) The evolution of the raw temperature profile (black lines) when a range of τ_T is applied (blue lines) to find the optimal thermistor thermal mass correction (red line) while profiling at 0.05 m s^{-1}. Mean temperature in the bottom layer is noted as a vertical gray line. (b) As in (a) but for the first difference of the temperature profile. (c) Quantified symmetry between the upper and lower layers (blue curve) as τ_T varies, with the optimal value that maximizes interface symmetry noted (red circle).

temperature at sample n. Coefficients a and b are functions of the initial error α, the time constant τ_{CTM}, and the sampling-frequency f_s, where

$$a = 2f_s\alpha\tau_{\mathrm{CTM}}(1 + 2f_s\tau_{\mathrm{CTM}})^{-1} \quad \text{and} \tag{4}$$

$$b = 1 - 2a\alpha^{-1}. \tag{5}$$

The difference between the temperature of the fluid as measured by the thermistor and the temperature of the conductivity cell is proportional to $\alpha \times \tau_{\mathrm{CTM}}$. For a CTD profiling at a constant speed $\alpha \times \tau_{\mathrm{CTM}}$ is equal to a constant, indicating there are a range of α and τ_{CTM} that can be used to correct for cell thermal mass. Therefore, two conditions are need to determine the optimal correction coefficients. To do this, we exploit the expected shape of the salinity interface between the upper and lower layers.

As described in section 4a, the idealized temperature and salinity profiles can be described by a Gauss error function whose thickness is determined by the difference in the properties between the upper and lower layers and the rate of diffusion. Although the temperature interface is symmetrical enough to exploit this characteristic to determine the thermistor thermal mass coefficients, a similar method cannot not be used to determine the conductivity cell thermal mass coefficients. There is a slight asymmetry to the salinity gradient caused by other mixing processes which are larger than the change in shape caused by the cell thermal mass. Applying the cell thermal mass correction changes the shape of the salinity gradient, but not enough to override the asymmetry. However, the change in shape can still be used to determine the optimal cell thermal mass coefficients by satisfying two conditions: 1) the salinity in the interface approaches the salinity in the lower layer, and 2) the salinity is constant in the lower layer (Fig. 4).

The first condition to determine the optimal cell thermal mass correction coefficients is to match the interface salinity with the lower-layer salinity (Fig. 4). This is done via an iterative method that minimizes the difference between the maximum salinity in the interface and the salinity in the lower layer, similar to the overshoot method used in the thermistor thermal mass time correction (Fig. 5). The optimal thermal mass coefficients that satisfy this condition fall along a line of the general form $\alpha = C_1\tau_{\mathrm{CTM}}^{-1} + C_2$, where C_1 and C_2 are determined by linear least squares regression.

The second condition is that the salinity below the interface must be constant. If the wrong α and τ_{CTM} are applied, the salinity in the interface will approach the lower-layer value but then rebound to a lower value (Fig. 4). By fitting a second-order polynomial using least squares regression to the salinity in the lower layer, ''curviness'' can be quantified (Fig. 5). The fit that minimizes the magnitude of the second-order

TABLE 1. Correction coefficients for pumped SBE 41CP sampling at 16 Hz determined from the stratified tank experiment.

Profile no.	Profiling speed (m s^{-1})	f_s (Hz)	τ_T (s)	t_P (s)	α	τ_{CTM} (s)
3	0.05	16	0.47	0	0.038	16.5
5	0.10	16	0.47	0.1250	0.050	7.6
6	0.15	16	0.50	0.1250	0.095	3.6

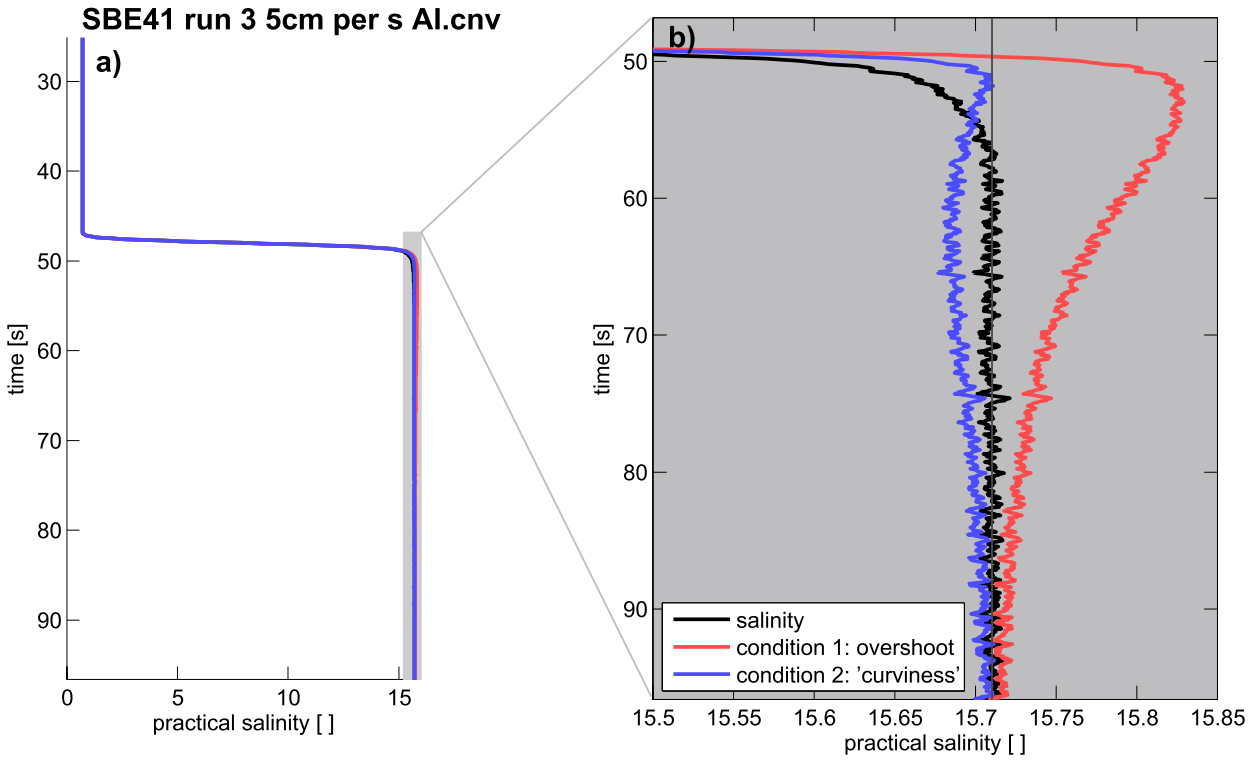

FIG. 4. (a) Salinity profile with optimized (black curve) and nonoptimized (red and blue curves) cell thermal mass correction coefficients applied. (b) If incorrect α and τ_{CTM} are applied, the salinity in the interface will either overshoot (red curve) or undershoot (not shown) the lower layer or relax to a value below the lower-layer salinity, i.e., be "curvy" (blue curve).

coefficient has the least rebound and gives the best approximation of a homogeneous lower layer. Applying these two conditions produced reasonable values of the coefficients α and τ_{CTM} for the three pumped profiles (Table 1). The corrected profiles have a sharp interface, a maximum salinity in the interface that matches the salinity in the lower layer, and a uniform bottom layer (Fig. 6). As the profiling speed increases, τ_{CTM} decreases due to increased flow through and around the glass cell and urethane jacket, thinning the boundary layer, increasing thermal conduction, and resulting in a faster response. Conversely, α increases with profiling speed. This is contrary to results found in Morison et al. (1994), which found that α decreases with profiling speed. This may be an artifact of the numerical approximation used in the correction. It may be sensitive to sampling resolution which is amplified by the exceptionally large gradients in the tank.

Another method to identify the optimal values of α and τ_{CTM} is to examine the difference in the area between the corrected and uncorrected salinity curves, which is proportional to $\alpha \times \tau_{CTM}$. This method was tested and produced similar results to condition 1, but tended to produce coefficients that overcorrected salinity, resulting in profiles where the interface salinity overshot salinity in the lower layer.

5. Subsampling at 1 Hz

The stratified tank data were obtained at 16 Hz, but in practice the SBE 41CP samples at 1 Hz. Therefore, the corrections must be modified for 1-Hz sampling so that they can be used for processing on board Argo floats. The operational Argo coefficients are determined by subsampling the 16-Hz stratified tank data to mimic a SBE 41CP sampling at 1 Hz, recomputing the correction coefficients by iterating through a range of corrections, applying the correction to the 1-Hz data, and then minimizing the difference between 16-Hz data. Subsampling provides sixteen 1-Hz realizations for each profile, and the operational Argo correction is taken as the mean of the realizations.

Although subsampling gives corrections to be used in situ, accuracy is reduced as sampling resolution decreases. When sampling at 1 Hz in the stratified tank, sampling distance is on the order of the gradient thickness so that for each realization there are typically only 1–2 samples within the interface. Even when the corrections are optimized, the subsampled 1-Hz data will

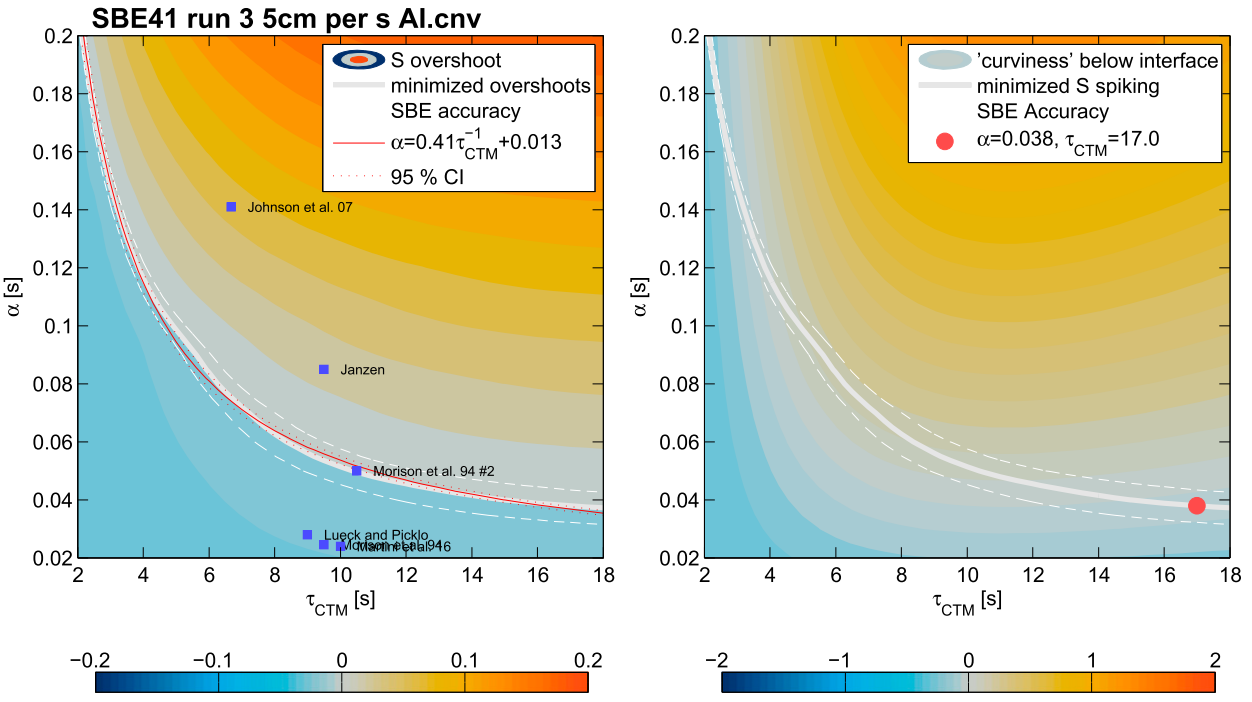

FIG. 5. Estimated cell thermal mass coefficients for the 0.05 m s^{-1}: (left) the plot to find the coefficients that match condition 1 and (right) the application of condition 2.

never match the 16-Hz values. This should be taken into consideration when corrections are determined from stratified tank data.

a. In situ SBE 41CP sampling

The SBE 41CP samples temperature, pressure, and conductivity in a sequence and is reported at the end of the 1-s sampling interval. Within each second, temperature is sampled from 0 to 215 ms, pressure from 215 to 317 ms, pressure temperature from 317 to 396 ms, and conductivity from 410 to 520 ms. The remaining 480 ms are processing time, and the samples are reported at the end of the second. To mimic SBE 41CP sampling, the 16-Hz data are interpolated onto a 1-ms time grid, bin averaged into the aforementioned sampling periods, and reported every second. This is done so that the corrections to the 16-Hz data determined from the tank can be directly applied to floats.

b. 1-Hz thermistor thermal mass

The ideal thermistor time constants for floats sampling at 1 Hz are shorter than those found at 16 Hz to compensate for lower sampling resolution (Table 2). When the original 16-Hz coefficients are applied, the profile is overcorrected and interface temperatures overshoot the temperature of the lower layer.

The 1-Hz correction is smaller than the value of τ_T = 0.39 s found by Johnson et al. (2007) due to differences in methods used to apply the correction. In Johnson et al. (2007), 1-Hz data are interpolated onto a 100-Hz grid using a cubic spline, the correction is applied using the first difference of supersampled data [Eq. (1)], and then they are interpolated back to the original 1-Hz grid. Here, dT/dz is simply the backward first difference of the full-resolution or subsampled temperature data. When sampling at frequencies of >4 Hz, that is, at 16 Hz, the temperature data are lightly smoothed with an $(11/16 \times f_s)$-point Hanning filter before taking the first difference to reduce the effect of instrument noise on the correction. The first difference correction method presented here may be preferred for use on board the SBE 41CP before bin averaging because it is still valid at coarser resolutions and computationally more efficient.

c. 1-Hz temperature and conductivity alignment

The subsampled temperature and conductivity data are aligned by first applying the thermistor thermal mass correction to the subsampled temperature, then determining the optimal lag time by linear interpolation. Optimized lags for the subsampled data are all negative, indicating that temperature *lags* conductivity. This is atypical for pumped and ducted CTDs, where conductivity lags concurrently sampled temperature due to the length of time it takes for a water parcel to travel between the sensors.

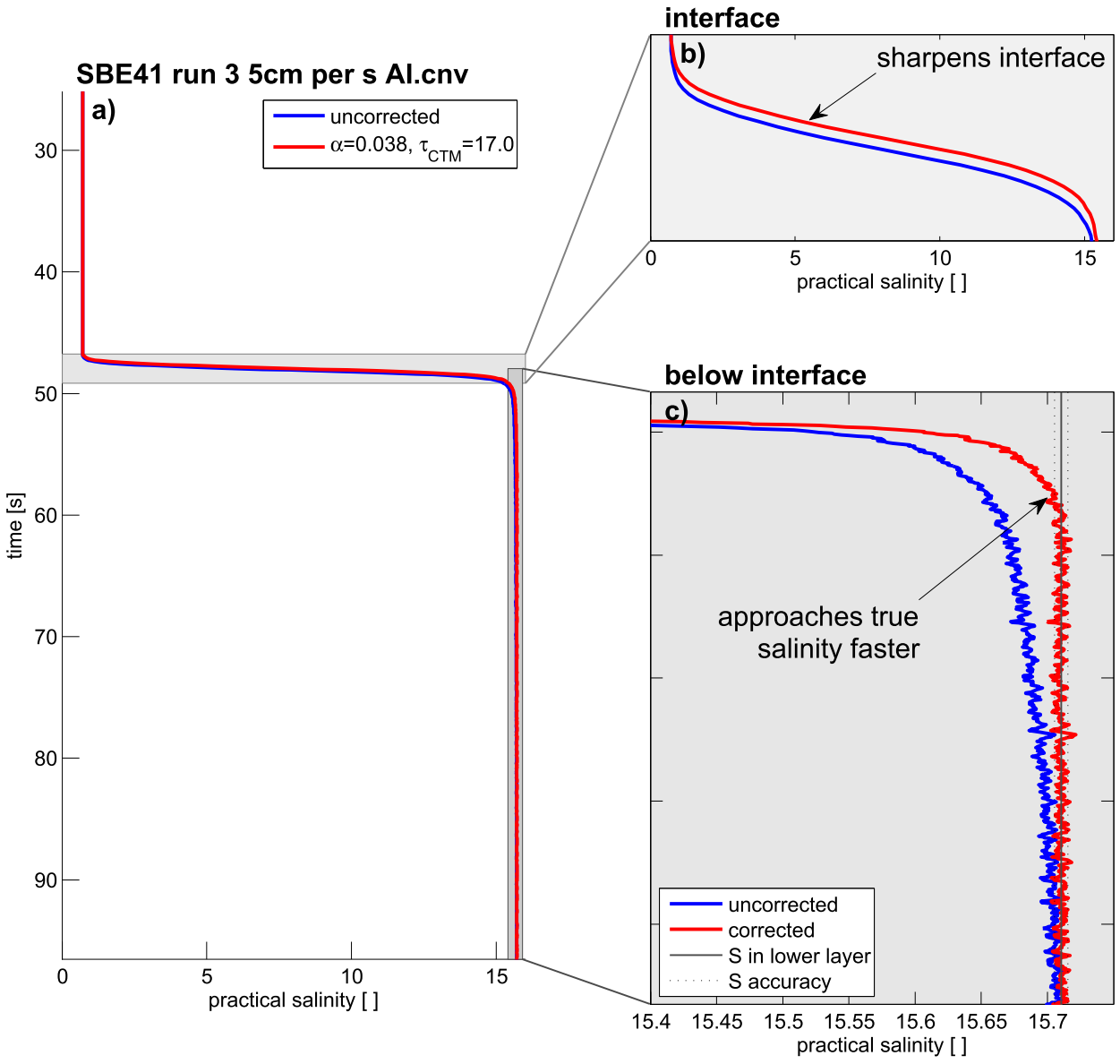

FIG. 6. (a) Comparison of salinity uncorrected (blue curves) and corrected (red curves) for conductivity cell thermal mass. When the plot is enlarged, one can see more clearly how the correction (b) sharpens the salinity interface and (c) causes the lower-layer value to be approached faster.

In the subsampled data, negative lags are caused by asynchronous sampling (conductivity is sampled 195 ms after temperature). The gap between the temperature and conductivity samples is too long. Water sampled by the conductivity sensor has passed the thermistor before it makes a measurement. In other words, when profiling upward (downward), the conductivity cell is sampling a shallower (deeper) water parcel than the thermistor. The lag lengthens as profiling speed increases, indicating water parcels travel through the duct faster as profiling speed increases. Water in the duct is propelled by induced flow within the CTD plumbing due to the orientation of the TC duct inlet and outlet in the ambient flow.

d. 1-Hz conductivity cell thermal mass

Before subsampled conductivity cell thermal mass coefficients are estimated, the thermistor thermal lag correction must be applied and temperature and conductivity aligned using the previously determined 1-Hz corrections. For each realization, there is a range of α and τ_{CTM} that minimizes the difference between

TABLE 2. Correction coefficients for pumped SBE 41CP sampling at 1 Hz determined from subsampling 16-Hz data from the stratified tank experiment.

Profile no.	Profiling speed ($m\,s^{-1}$)	f_s (Hz)	τ_T (s)	t_P (s)	α	τ_{CTM} (s)
3	0.05	1	0.21	−0.19	0.027	16.3
5	0.10	1	0.16	−0.26	0.078	11.0
6	0.15	1	0.23	−0.25	0.150	6.6

the 16- and the 1-Hz subsampled salinity (Fig. 7). This range falls upon a curve that lies close to the 16-Hz correction coefficient curve in Fig. 5. The optimal coefficient is chosen as the value on the mean curve closest to the 16-Hz value. The optimized 1-Hz coefficients are close in value to the 16-Hz coefficients (Table 2). Differences between the 1- and 16-Hz coefficients are attributed to poor interface resolution when sampling at a lower frequency, leading to salinity errors as large as 2.5 PSU.

The thermistor thermal lag must be corrected before iterating to solve for the conductivity thermal lag. If not, each realization produces a minimization curve that is even further offset from the optimal 16-Hz values. For the 0.10 and 0.15 $m\,s^{-1}$ profiles there are no values of α and τ_{CTM} estimated with uncorrected temperature data that could be applied to the 1-Hz salinity to match the 16-Hz salinity. In practice, this suggests correction coefficients may be difficult to estimate due to unexplained variability caused when the thermistor thermal mass correction is not applied.

6. Conclusions

Profiling experiments within a two-layer stratified tank are used to determine dynamic corrections for SBE 41CP CTDs deployed on autonomous Argo floats. Within the stratified tank, large temperature ($dT \approx 6°C$) and salinity ($dS \approx 16$) gradients over distances of less than 10 cm amplify dynamic sensor errors, enabling their correction. Corrections for thermistor thermal mass, temperature and conductivity mismatch, and conductivity cell thermal mass improve practical salinity accuracy up to 2.18, or 14% of the net gradient in the tank when sampling at 16 Hz.

Subsampled 16-Hz data are used to determine practical corrections for use on Argo floats sampling at 1 Hz. Corrections to 1-Hz data sharpen vertical gradients, reduce spiking, and improve practical salinity accuracy up to 0.95 or 6% of the net gradient (Fig. 8). Spikes in uncorrected data are primarily caused by the mismatch in temperature and conductivity sampling, and corrected when the data profiles are aligned.

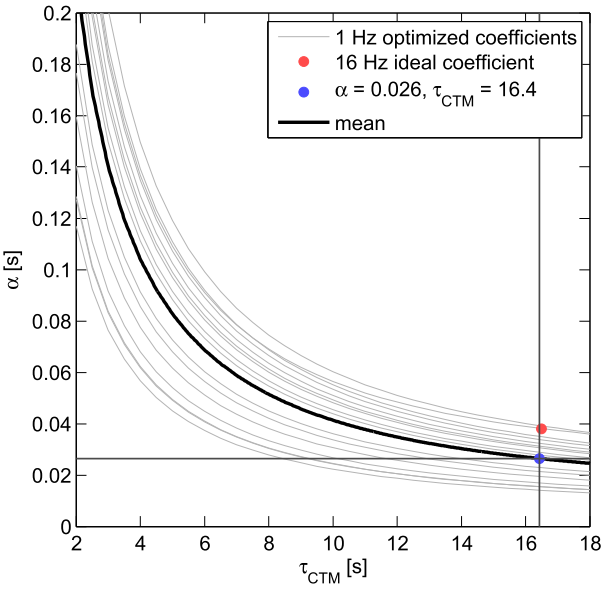

FIG. 7. Conductivity cell thermal mass correction coefficients for the 16-Hz full-resolution (red dot) and 1-Hz subsampled data (blue dot) when profiling at 0.05 $m\,s^{-1}$. The range of 1-Hz coefficients for each realization that best reproduce the 16 Hz data is shown by the gray curves. The mean is shown by the black curve.

Each dynamic correction improves salinity accuracy differently. The thermistor thermal mass correction improves accuracy within the interface by matching the thermistor response time to the conductivity cell response time. Alignment improves accuracy within the interface by matching temperature and conductivity samples. The cell thermal mass correction improves accuracy in the bottom layer by approaching the true salinity faster. Of these three corrections, aligning temperature and conductivity leads to the greatest improvement in accuracy in the stratified tank. This should be taken into consideration when determining which corrections to apply to in situ float data.

When deployed, the SBE 41CP computes salinity on board and returns pressure, temperature, and salinity binned onto a 1-m grid. If these corrections are to be applied, this must be done in the firmware before the data are binned and telemetered back to the user. Average ascent rates for the Argo fleet is 0.10 $m\,s^{-1}$. If corrections determined from the stratified tank profiles are to be used, use those that match the average ascent rate of the Argo fleet. The following corrections should be applied in order as follows:

1) Apply thermistor thermal mass correction to temperature, where $\tau_T = 0.16$ s.
2) Align temperature and conductivity data using a lag of $t_p = -0.26$ s.

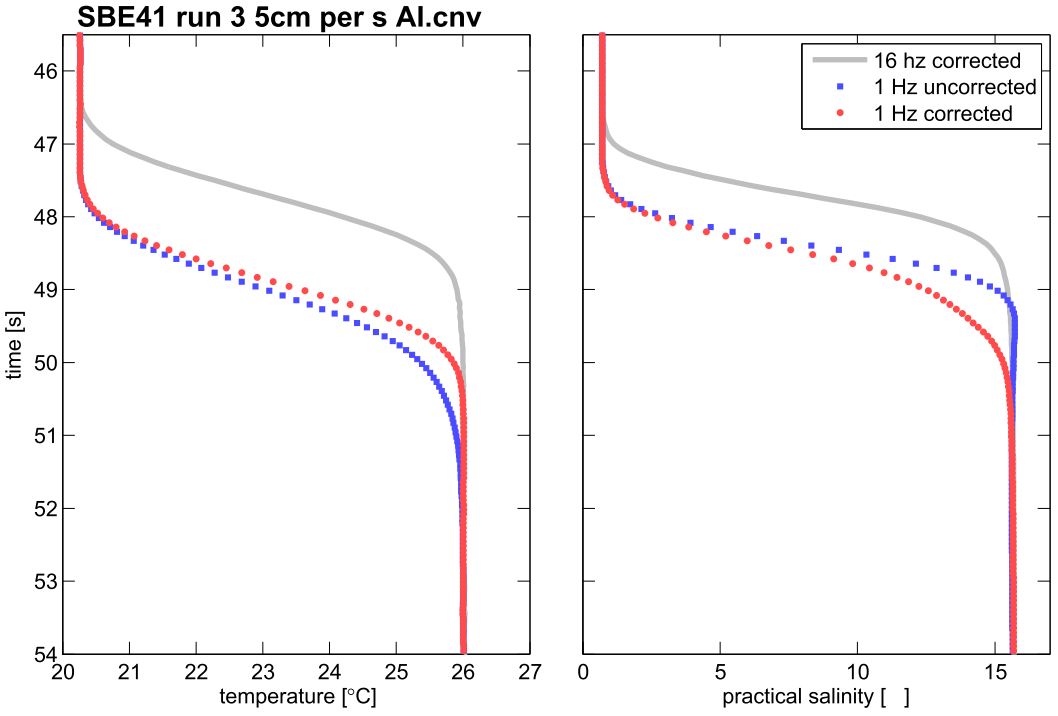

FIG. 8. (left) Temperature and (right) salinity 16-Hz profiles with all corrections applied (gray curves), discrete 1-Hz subsampled realizations with no corrections applied (blue dots), and discrete 1-Hz subsampled realizations with all corrections applied (red dots). The subsampled data are plotted when reported at the end of the sampling interval and lag the 16-Hz data by 1 s. Uncorrected 1-Hz salinity appears to lead the corrected 1-Hz salinity because conductivity is sampled approximately 0.4 s after temperature because of the gap between temperature and conductivity sampling.

3) Apply conductivity cell thermal mass correction following Lueck and Picklo (1990) or Morison et al. (1994), where $\alpha = 0.078$ and $\tau_{CTM} = 11.0$ s.

If sensor response times are long, thermal mass errors can persist into subsequent bins when profiling. On Argo floats, the SBE 41CP thermistor and conductivity cell thermal mass time constants are shorter than the 20, 10, and 5 s it takes to sample a 1-m bin at 0.05, 0.1, and 0.2 m s^{-1}, respectively. In addition, in situ data show that the buoyancy-driven floats slow or even stall when encountering regions of high vertical stratification. Although response times increase at slow vertical ascent speeds, they are still shorter than the time the sensors spend in the gradient. Only if the gradient is found at the upper depth of the bin can the error carry over. Therefore, cell thermal mass errors are isolated to one to two bins.

The stratified tank experiments are a highly controlled environment, with a well-defined stratification jump maintained by diffusion measured at a constant profiling speed. This is not the case in the open ocean. Profiling speeds vary, changing the optimal correction coefficients. If applied to in situ data, the corrections could improve data accuracy. However, if the wrong corrections are applied there is a risk of introducing additional error. Further experiments using in situ data from CTDs returning data at 1 Hz are planned to verify the corrections presented here and provide guidance for future corrections on board Argo floats.

Acknowledgments. The authors thank Breck Owens and the Argo steering team for encouraging and supporting this research. We also thank the anonymous reviewer whose comments improved the paper.

REFERENCES

Fofonoff, N. P., S. P. Hayes, and R. C. Millard, 1974: WHOI/Brown CTD microprofiler: Methods of calibration and data handling. Woods Hole Oceanographic Institution Tech. Rep., 72 pp., https://doi.org/10.1575/1912/647.

Horne, E. P. W., and J. M. Toole, 1980: Sensor response mismatches and lag correction techniques for temperature-salinity profilers. *J. Phys. Oceanogr.*, **10**, 1122–1130, https://doi.org/10.1175/1520-0485(1980)010<1122:SRMALC>2.0.CO;2.

Johnson, G. C., J. M. Toole, and N. G. Larson, 2007: Sensor corrections for Sea-Bird SBE-41CP and SBE-41 CTDs. *J. Atmos.*

Oceanic Technol., **24**, 1117–1130, https://doi.org/10.1175/JTECH2016.1.

Lueck, R. G., 1990: Thermal inertia of conductivity cells: Theory. *J. Atmos. Oceanic Technol.*, **7**, 741–755, https://doi.org/10.1175/1520-0426(1990)007<0741:TIOCCT>2.0.CO;2.

——, and J. J. Picklo, 1990: Thermal inertia of conductivity cells: Observations with a Sea-Bird cell. *J. Atmos. Oceanic Technol.*, **7**, 756–768, https://doi.org/10.1175/1520-0426(1990)007<0756:TIOCCO>2.0.CO;2.

Morison, J., R. Anderson, N. Larson, E. D'Asaro, and T. Boyd, 1994: The correction for thermal-lag effects in Sea-Bird CTD data. *J. Atmos. Oceanic Technol.*, **11**, 1151–1164, https://doi.org/10.1175/1520-0426(1994)011<1151:TCFTLE>2.0.CO;2.

Schmitt, R. W., R. C. Millard, J. M. Toole, and W. D. Wellwood, 2005: A double-diffusive interface tank for dynamic-response studies. *J. Mar. Res.*, **63**, 263–289, https://doi.org/10.1357/0022240053693842.